Calculation of the Scattering Function $S(\mathbf{k},\omega)$ for the Inelastic Scattering of Neutrons by Anharmonic Crystals*

A. A. MARADUDIN
Westinghouse Research Laboratories, Pittsburgh, Pennsylvania

AND

V. AMBEGAOKAR†
Department of Physics and Laboratory of Atomic and Solid State Physics, Cornell University, Ithaca, New York

(Received 25 March 1964)

A numerical calculation is presented of van Hove's scattering function $S(\mathbf{k},\omega)$, which describes the inelastic scattering of neutrons by an anharmonic crystal with the transfer of momentum $\mathbf{k}$ and energy ω from neutron to crystal. Two contributions to $S(\mathbf{k},\omega)$ are included in the present calculation: the leading term which describes the broadening and shift of the one-phonon peak, and the leading term which describes the interference between the one-phonon peak and the diffuse multiphonon background. The calculations of $S(\mathbf{k},\omega)$ as a function of ω for fixed $\mathbf{k}$ are carried out in the high-temperature limit for a nearest-neighbor, central-force model of a face-centered cubic crystal which is chosen to approximate lead. The ω dependence of the phonon frequency shift and width, as well as of the coefficient of the interference term, is taken into account in these calculations. In the cases treated in the present paper the interference terms represent only a very small correction to the one-phonon peak, in agreement with a previous crude estimate by Ambegaokar, Conway, and Baym.

1. INTRODUCTION

THE theory of the inelastic scattering of neutrons by an anharmonic crystal has been the subject of several recent investigations.[1–9] Most of the interest has centered on the so-called "one-phonon peak" in the scattering cross section, which is that part of the cross section which describes the scattering of a neutron by the crystal with the excitation or de-excitation of one quantum of vibrational energy. It is this part of the cross section which displays most dramatically the effects of lattice anharmonicity on the phonons. A delta function in the harmonic approximation, centered at the frequency of the normal mode from which the neutrons are being scattered, the one-phonon peak in an anharmonic crystal is shifted in position and broadened in comparison.

In a recent paper[9] by Conway, Baym, and one of the present authors (V.A.), it was pointed out that the anharmonic forces in a crystal, in addition to broadening and shifting the one-phonon peaks, lead to an interference between the one-phonon peak and the diffuse multiphonon background. It was shown that the sum of the one-phonon peak and the interference terms obeys a sum rule, and a crude numerical estimate of the ratio of the amplitudes of the asymmetrical interference terms and the symmetrical peaked terms was made which indicated that under typical conditions in lead the asymmetry might amount to a few percent.

In the present paper we present a numerical calculation of van Hove's[10] scattering function $S(\mathbf{k},\omega)$, which is related to the differential scattering cross section per unit solid angle per unit interval of energy of the scattered neutron by

$$d^2\sigma/d\Omega d\epsilon = a^2(q_f/q_i)S(\mathbf{k},\omega). \tag{1.1}$$

In this equation, a is the nuclear scattering length, $\mathbf{q}_i$ is the initial wave vector of the neutron and $\mathbf{q}_f$ is its final wave vector, $\mathbf{k}=\mathbf{q}_i-\mathbf{q}_f$ is the momentum transfer from neutron to crystal, and $\omega=(q_i^2-q_f^2)/2m$, where m is the neutron mass, is the energy transfer from neutron to crystal (we use units such that $\hbar=1$). In the present calculation we include both of the contributions to $S(\mathbf{k},\omega)$ mentioned in the preceding paragraph: the one-phonon peak and the leading term which describes the interference between the one-phonon peak and the multiphonon background. Although, as we have mentioned, the contribution of the latter term is expected to be small, it seems to us not without interest to verify this expectation by a detailed calculation. The calculations will be carried out in the high-temperature limit for a nearest-neighbor, central force model of a face-centered cubic crystal which we will use to approximate lead.

* This research was supported by the Advanced Research Projects Agency, Director for Materials Sciences and was technically monitored by the U. S. Air Force Office of Scientific Research under Contract AF 49(638)-1245.

† Alfred P. Sloan Foundation Fellow.

[1] L. van Hove, N. M. Hugenholtz, and L. P. Howland, *Quantum Theory of Many-Particle Systems* (W. A. Benjamin, Inc., New York, 1961), pp. 1–101.

[2] V. N. Kashcheev and M. A. Krivoglaz, Fiz. Tverd. Tela **3**, 1528 (1960) [English transl.: Soviet Phys.—Solid State **3**, 1107 (1961)].

[3] G. Baym, Phys. Rev. **121**, 741 (1961).

[4] J. J. J. Kokkedee, Physica **28**, 374 (1962).

[5] A. A. Maradudin and A. E. Fein, Phys. Rev. **128**, 2589 (1962).

[6] A. A. Maradudin, A. E. Fein, and G. H. Vineyard, Phys. Stat. Solidi **2**, 1479 (1962).

[7] A. A. Maradudin, Phys. Stat. Solidi **2**, 1493 (1962).

[8] B. V. Thompson, Phys. Rev. **131**, 1420 (1963).

[9] V. Ambegaokar, J. Conway, and G. Baym, *Proceedings of the 1963 International Conference on Lattice Dynamics* (Pergamon Press, Inc., New York, 1964). This paper will be referred to as I in the remainder of this article.

[10] L. van Hove, Phys. Rev. **95**, 249 (1954).

Calculations of $S(\mathbf{k},\omega)$ have recently been carried out by Cowley[11] for the optical modes at $\mathbf{k}=0$ in sodium iodide and potassium bromide. Only the contribution from the one-phonon peak was included in Cowley's calculations.

Because the theory of the one-phonon peak has been discussed extensively in the literature,[1-9] in the following two sections we concentrate our attention on the asymmetric interference term.[9]

2. ANALYTICAL DEVELOPMENT

In this section we shall first briefly summarize the formulation given in I. Then we shall develop the formulas for the interference term in the first order of the interaction between "dressed" phonons.

The cross section for the scattering of a neutron by a Bravais crystal with energy loss ω and momentum loss $\mathbf{k}$[12] is proportional to [Eq. (2.9) of I]

$$2\pi S(\mathbf{k},\omega)=\frac{2\,\mathrm{Im}C(\mathbf{k},\,\omega-i\epsilon)}{1-e^{-\beta\omega}}. \tag{2.1}$$

Here $C(\mathbf{k},z)$ is the continuation to the complex z plane of the Fourier series coefficients

$$C(\mathbf{k},\nu_m)=\int_0^{-i\beta} C(\mathbf{k},t)e^{i\nu_m t}dt, \quad \nu_m=2\pi im/\beta,$$

of the correlation function

$$C(\mathbf{k},t)=-i\sum_{\mathbf{gh}} e^{-i\mathbf{k}\cdot(\mathbf{g}-\mathbf{h})}\langle T[e^{-i\mathbf{k}\cdot\boldsymbol{\phi}_\mathbf{g}(t)}e^{i\mathbf{k}\cdot\boldsymbol{\phi}_\mathbf{h}(0)}]\rangle. \tag{2.2}$$

In this equation $\mathbf{g}$ and $\mathbf{h}$ run over the lattice sites of the crystal, N is the number of atoms in the crystal, t is restricted to the region $\mathrm{Re}t=0$, $-\beta<\mathrm{Im}t<0$, T orders operators from right to left in order of increasing negative imaginary t, $\boldsymbol{\phi}_\mathbf{g}(t)$ is the Heisenberg representation operator for the excursion of the atom at the site $\mathbf{g}$, and the expectation value is in the canonical ensemble for the anharmonic crystal. It was shown in I, by a rearrangement of the power-series expansion of Eq. (2.2) in $\mathbf{k}$, that this equation could be put in the form [Eq. (2.22) of I]

$$C(\mathbf{k},t)=-i[d(\mathbf{k})]^2\sum_{\mathbf{gh}} e^{-i\mathbf{k}\cdot(\mathbf{g}-\mathbf{h})}\times\exp\{\langle T(\exp[-i\mathbf{k}\cdot\boldsymbol{\phi}_\mathbf{g}(t)]-1)\times(\exp[i\mathbf{k}\cdot\boldsymbol{\phi}_\mathbf{h}(0)]-1)\rangle_L\}. \tag{2.3}$$

Here $[d(\mathbf{k})]^2$ is the Debye-Waller factor given by

$$d(\mathbf{k})=\langle\exp i(\mathbf{k}\cdot\boldsymbol{\phi})\rangle=\exp[\langle\exp i(\mathbf{k}\cdot\boldsymbol{\phi})\rangle_L-1]. \tag{2.4}$$

The symbol $\langle\ \rangle_L$ in Eqs. (2.3) and (2.4) means the linked or cumulant average.[13] For example,

$$\langle T\boldsymbol{\phi}_\mathbf{g}^2(t)\boldsymbol{\phi}_\mathbf{h}(0)\rangle_L=\langle T\boldsymbol{\phi}_\mathbf{g}^2(t)\boldsymbol{\phi}_\mathbf{h}(0)\rangle-\langle\boldsymbol{\phi}_\mathbf{g}^2(t)\rangle\langle\boldsymbol{\phi}_\mathbf{h}(0)\rangle-2\langle T\boldsymbol{\phi}_\mathbf{g}(t)\boldsymbol{\phi}_\mathbf{h}(0)\rangle\langle\boldsymbol{\phi}_\mathbf{g}(t)\rangle+2\langle\boldsymbol{\phi}_\mathbf{g}(t)\rangle^2\langle\boldsymbol{\phi}_\mathbf{h}(0)\rangle. \tag{2.5}$$

From the point of view of graphical perturbation theory, the cumulant average implies that one must consider only graphs in which, in every order, all displacement operators are linked.

The decomposition of the cross section into the elastic, one-phonon, and multiphonon terms follows from Eq. (2.3) by an expansion in powers of the curly bracket. The zero-order term gives the elastic scattering, and that part of the first-order term in which a single true phonon state occurs as a real intermediate state gives rise to the one-phonon peak. The interference terms also come from the first-order term and correspond to processes in which a multiphonon excitation is on the energy shell, but a single-phonon state occurs virtually at an earlier or later stage of the process and is coupled coherently to the many-phonon excitation.

We are concerned in this paper with the evaluation of the lowest order contribution to the interference term for a crystal with cubic anharmonicities. This contribution occurs in the terms

$$\tilde{C}(\mathbf{k},t)=-i[d(\mathbf{k})]^2\sum_{\mathbf{gh}} e^{-i\mathbf{k}\cdot(\mathbf{g}-\mathbf{h})}\times\left\{\left\langle T\frac{1}{2!}[-i\mathbf{k}\cdot\boldsymbol{\phi}_\mathbf{g}(t)]^2[i\mathbf{k}\cdot\boldsymbol{\phi}_\mathbf{h}(0)]\right\rangle_L+\left\langle T[-i\mathbf{k}\cdot\boldsymbol{\phi}_\mathbf{g}(t)][i\mathbf{k}\cdot\boldsymbol{\phi}_\mathbf{h}(0)]^2\frac{1}{2!}\right\rangle_L\right\}. \tag{2.6}$$

We shall see from symmetry considerations that the two terms in the bracket make equal contributions for a Bravais crystal, to which we limit ourselves in this paper. The explicit proof is as follows: From time reversal invariance we have that

$$F_\mathbf{gh}(t)=\langle[\mathbf{k}\cdot\boldsymbol{\phi}_\mathbf{g}(t)]^2[\mathbf{k}\cdot\boldsymbol{\phi}_\mathbf{h}(0)]\rangle=\langle[\mathbf{k}\cdot\boldsymbol{\phi}_\mathbf{h}(0)][\mathbf{k}\cdot\boldsymbol{\phi}_\mathbf{g}(-t)]^2\rangle. \tag{2.7}$$

Now, using the translational invariance of the lattice and invariance under translations of time, we have

$$F_\mathbf{gh}(t)=\langle[\mathbf{k}\cdot\boldsymbol{\phi}_{-\mathbf{g}}(t)][\mathbf{k}\cdot\boldsymbol{\phi}_{-\mathbf{h}}(0)]^2\rangle. \tag{2.8}$$

Finally, we use the inversion symmetry of a Bravais lattice, i.e., invariance under the transformation $\boldsymbol{\phi}_\mathbf{h}\rightarrow-\boldsymbol{\phi}_{-\mathbf{h}}$, to obtain

$$F_\mathbf{gh}(t)=-\langle[\mathbf{k}\cdot\boldsymbol{\phi}_\mathbf{g}(t)][\mathbf{k}\cdot\boldsymbol{\phi}_\mathbf{h}(0)]^2\rangle. \tag{2.9}$$

[11] R. A. Cowley, *Proceedings of the 1963 International Conference on Lattice Dynamics* (Pergamon Press, Inc., New York, 1964).

[12] In this paper we adopt the convention that the wave vector $\mathbf{k}$ is reserved for the momentum loss from neutron to crystal and that the phonon wave vector is $\mathbf{q}$.

[13] M. G. Kendall and A. Stuart, *The Advanced Theory of Statistics* (Charles Griffin and Company, Ltd., London, 1958), Chap. 3.

The equality of the two terms in (2.6) then follows.[14]

We have now to evaluate $\tilde{C}(\mathbf{k},t)$ in perturbation theory. The anharmonic contribution to the Hamiltonian may be written in the form

$$H_3=\frac{1}{3!}\sum_{\mathbf{q}_1 j_1}\sum_{\mathbf{q}_2 j_2}\sum_{\mathbf{q}_3 j_3} B(\mathbf{q}_1 j_1;\mathbf{q}_2 j_2;\mathbf{q}_3 j_3) \times Q(\mathbf{q}_1 j_1)Q(\mathbf{q}_2 j_2)Q(\mathbf{q}_3 j_3), \quad (2.10)$$

where $Q(\mathbf{q}j)$ is the coordinate of a phonon of wave vector $\mathbf{q}$ and polarization j. $Q(\mathbf{q}j)$ is related to the displacement vector $\boldsymbol{\phi}_\mathbf{g}$ by

$$\boldsymbol{\phi}_\mathbf{g}=\frac{1}{(N)^{1/2}}\sum_{\mathbf{q}j}\boldsymbol{\varepsilon}(\mathbf{q}j)Q(\mathbf{q}j)e^{i\mathbf{q}\cdot\mathbf{g}}, \quad (2.11)$$

where $\boldsymbol{\varepsilon}(\mathbf{q}j)$ is a polarization vector. In terms of the usual phonon creation and destruction operators it is given by

$$Q(\mathbf{q}j)=(\hbar/2M\omega_{\mathbf{q}j})^{1/2}(b_{-\mathbf{q}j}{}^\dagger+b_{\mathbf{q}j}), \quad (2.12)$$

where M is the mass of an atom and $\omega_{\mathbf{q}j}$ is the frequency of the phonon $(\mathbf{q}j)$. The coefficient B is given in terms of the cubic anharmonic force constant $\Phi_{\alpha\beta\gamma}(\mathbf{g}\mathbf{g}'\mathbf{g}'')$ of Born and Huang[15] by

$$B(\mathbf{q}_1 j_1;\mathbf{q}_2 j_2;\mathbf{q}_3 j_3)=\frac{1}{N^{3/2}}\sum_{\mathbf{g}\mathbf{g}'\mathbf{g}''}\sum_{\alpha\beta\gamma}\Phi_{\alpha\beta\gamma}(\mathbf{g}\mathbf{g}'\mathbf{g}'')\mathcal{E}_\alpha(\mathbf{q}_1 j_1) \times\mathcal{E}_\beta(\mathbf{q}_2 j_2)\mathcal{E}_\gamma(\mathbf{q}_3 j_3)e^{i(\mathbf{q}_1\cdot\mathbf{g}+\mathbf{q}_2\cdot\mathbf{g}'+\mathbf{q}_3\cdot\mathbf{g}'')}. \quad (2.13)$$

It vanishes unless $\mathbf{q}_1+\mathbf{q}_2+\mathbf{q}_3$ equals 2π times a vector of the reciprocal lattice. If we make use of the fact that $\Phi_{\alpha\beta\gamma}(gg'g'')$ changes its sign under the inversion operation,

$$\Phi_{\alpha\beta\gamma}(-\mathbf{g}-\mathbf{g}'-\mathbf{g}'')=-\Phi_{\alpha\beta\gamma}(\mathbf{g}\mathbf{g}'\mathbf{g}''), \quad (2.14)$$

we can show that $B(\mathbf{q}_1 j_1;\mathbf{q}_2 j_2;\mathbf{q}_3 j_3)$ is purely imaginary.

In the first order of perturbation theory we have [using the equality of the two terms on the right side of Eq. (2.6)]

$$\tilde{C}(\mathbf{k},t)=-[d(\mathbf{k})]^2\sum_{\mathbf{g}\mathbf{h}}e^{-i\mathbf{k}\cdot(\mathbf{g}-\mathbf{h})} \times(-i)\int_0^{-i\beta}dt'\langle T\{[\mathbf{k}\cdot\boldsymbol{\phi}_\mathbf{g}(t)]^2 \times H_3(t')[\mathbf{k}\cdot\boldsymbol{\phi}_\mathbf{h}(0)]\}\rangle, \quad (2.15)$$

where the time dependence of operators and the thermal average are now governed by the harmonic part of the Hamiltonian. Substituting the expression (2.10) for H_3 into Eq. (2.15) and using Wick's theorem, we get, using Eq. (2.11),

$$\tilde{C}(\mathbf{k},t)=\frac{[d(\mathbf{k})]^2}{N^{3/2}}\sum_{\mathbf{g}\mathbf{h}}\sum_{\mathbf{q}_1\mathbf{q}_2\mathbf{q}_3}\sum_{j_1 j_2 j_3}e^{-i\mathbf{k}\cdot(\mathbf{g}-\mathbf{h})}e^{i(\mathbf{q}_1\cdot\mathbf{g}+\mathbf{q}_2\cdot\mathbf{g}-\mathbf{q}_3\cdot\mathbf{h})}[\mathbf{k}\cdot\boldsymbol{\varepsilon}(\mathbf{q}_1 j_1)][\mathbf{k}\cdot\boldsymbol{\varepsilon}(\mathbf{q}_2 j_2)][\mathbf{k}\cdot\boldsymbol{\varepsilon}(-\mathbf{q}_3 j_3)] \times B(-\mathbf{q}_1 j_1;-\mathbf{q}_2 j_2;\mathbf{q}_3 j_3)\int_0^{-i\beta}dt' D_{\mathbf{q}_1 j_1}{}^0(t-t')D_{\mathbf{q}_2 j_2}{}^0(t-t')D_{\mathbf{q}_3 j_3}{}^0(t'). \quad (2.16)$$

In this equation $D_{\mathbf{q}j}{}^0(t)$ is the phonon Green's function in the harmonic approximation. In general, the Green's function is given by

$$D_{\mathbf{q}jj'}(t)=-i\langle T[Q_{\mathbf{q}j}(t)Q_{-\mathbf{q}j'}(0)]\rangle, \quad (2.17)$$

and because of polarization mixing it is not diagonal in j and j'. Although we could formally diagonalize $D_{\mathbf{q}jj'}(t)$, at the expense of introducing additional complications into the expressions which we will derive, this is not really necessary. For, to the lowest nonvanishing order in the anharmonic force constants, $D_{\mathbf{q}jj'}(t)$ is diagonal in j and j',[5] and this order is consistent with our use of first-order perturbation theory in obtaining $\tilde{C}(\mathbf{k},t)$. We denote the diagonal part of $D_{\mathbf{q}jj'}(t)$ by $D_{\mathbf{q}j}(t)$.

By including, together with Eq. (2.16), all graphs in which self-energy parts are added to the phonon lines, one obtains an expression identical to (2.16) but with the superscript zero removed. This formal summation is necessary in order that the calculated interference terms have the correct line shape. In calculating the amplitude of the term, however, one shall neglect the higher order effects due to finite phonon lifetimes.

After the phonon Green's functions in Eq. (2.16) have been "dressed," the Fourier coefficient of $\tilde{C}(\mathbf{k},t)$ may be written in terms of the Fourier coefficient of the Green's function

$$D(\nu_m)=\int_0^{-i\beta}D(t)e^{i\nu_m t}dt, \quad \nu_m=2\pi i m/\beta,$$

[14] This result contradicts a statement in a recent paper by Thompson (Ref. 8) to the effect that the contribution given by Eq. (2.6) vanishes because the two terms on the right side of the equation cancel. In a private communication to the authors, Dr. Thompson agrees that his statement is incorrect.

[15] M. Born and K. Huang, *Dynamical Theory of Crystal Lattices* (Oxford University Press, Oxford, 1954), p. 305.

as

$$\tilde{C}(\mathbf{k},\nu_m)=N^{1/2}[d(\mathbf{k})]^2\sum_{\mathbf{q}_1\mathbf{q}_2\mathbf{q}_3}\sum_{j_1j_2j_3}\Delta(\mathbf{k}-\mathbf{q}_3)B(-\mathbf{q}_1j_1;-\mathbf{q}_2j_2;\mathbf{q}_3j_3)[\mathbf{k}\cdot\boldsymbol{\varepsilon}(\mathbf{q}_1j_1)][\mathbf{k}\cdot\boldsymbol{\varepsilon}(\mathbf{q}_2j_2)][\mathbf{k}\cdot\boldsymbol{\varepsilon}(\mathbf{q}_3j_3)]$$
$$\times\frac{i}{\beta}\sum_{m'}D_{\mathbf{q}_1j_1}(\nu_m-\nu_{m'})D_{\mathbf{q}_2j_2}(\nu_{m'})D_{\mathbf{q}_3j_3}(\nu_m). \quad (2.18)$$

The function $\Delta(\mathbf{k}-\mathbf{q}_3)$ is defined by

$$\Delta(\mathbf{k}-\mathbf{q}_3)=\begin{cases}0 & \mathbf{k}\neq\mathbf{q}_3+\mathbf{K}_\nu,\\ 1 & \mathbf{k}=\mathbf{q}_3+\mathbf{K}_\nu,\end{cases}$$

where $\mathbf{K}_\nu$ is 2π times a vector of the reciprocal lattice. The Fourier coefficients of the Green's function have the well-known spectral representation

$$D_{\mathbf{q}j}(\nu_m)=\int_{-\infty}^{\infty}\frac{d\omega}{2\pi}\frac{A_{\mathbf{q}j}(\omega)}{\nu_m-\omega}. \quad (2.19)$$

After Eq. (2.19) is substituted in Eq. (2.18), the sum over m' may be performed by using the formula

$$\frac{i}{\beta}\sum_{m'}\frac{1}{\nu_m-\nu_{m'}-\omega_1}\frac{1}{\nu_{m'}-\omega_2}=-i\frac{N(\omega_2)-N(-\omega_1)}{\nu_m-\omega_1-\omega_2}, \quad (2.20)$$

where $N(\omega)=[\exp(\beta\omega)-1]^{-1}$. Finally, to calculate the contribution to the cross section one has to use Eq. (2.1). There are two contributions to $\mathrm{Im}C(\mathbf{k},\omega-i\epsilon)$. The first corresponds to putting the phonon labeled by $\mathbf{q}_3j_3$ in Eq. (2.18) on the energy shell. This term gives a correction to the amplitude of the one-phonon peak. The term of interest to us here comes from the vanishing of the energy denominator displayed in Eq. (2.20). From this part one obtains

$$2\,\mathrm{Im}\tilde{C}_{\mathrm{int}}(\mathbf{k},\omega-i\epsilon)=N^{1/2}[d(\mathbf{k})]^2\sum_{\mathbf{q}_1\mathbf{q}_2\mathbf{q}_3}\sum_{j_1j_2j_3}\Delta(\mathbf{k}-\mathbf{q}_3)\tilde{B}(-\mathbf{q}_1j_1;-\mathbf{q}_2j_2;\mathbf{q}_3j_3)[\mathbf{k}\cdot\boldsymbol{\varepsilon}(\mathbf{q}_1j_1)][\mathbf{k}\cdot\boldsymbol{\varepsilon}(\mathbf{q}_2j_2)][\mathbf{k}\cdot\boldsymbol{\varepsilon}(\mathbf{q}_3j_3)]$$
$$\times\int\frac{d\omega_1d\omega_2}{2\pi}A_{\mathbf{q}_1j_1}(\omega_1)A_{\mathbf{q}_2j_2}(\omega_2)\frac{N(-\omega_1)N(-\omega_2)}{N(-\omega)}\delta(\omega_1+\omega_2-\omega)P\int\frac{d\omega_3}{2\pi}\frac{A_{\mathbf{q}_3j_3}(\omega_3)}{\omega-\omega_3}. \quad (2.21)$$

In writing this result we have used the identity

$$N(-\omega_1)-N(\omega_2)=N(-\omega_1)N(-\omega_2)/N(-\omega_1-\omega_2). \quad (2.22)$$

In addition we have used the fact that B is purely imaginary to write $B=-i\tilde{B}$, where $\tilde{B}$ is real. We obtain from Eqs. (2.21) and (2.1) that the contribution to the cross section from the interference terms is proportional to

$$S_{\mathrm{int}}(\mathbf{k},\omega)=(N/2\pi)[d(\mathbf{k})]^2N(-\omega)\sum_j I_{\mathbf{k}j}(\omega)G_{\mathbf{k}j}(\omega), \quad (2.23)$$

where

$$I_{\mathbf{k}j}(\omega)=P\int(d\omega'/2\pi)[A_{\mathbf{k}j}(\omega')/(\omega-\omega')] \quad (2.24)$$

and

$$G_{\mathbf{k}j}(\omega)=-\frac{1}{(N)^{1/2}}\sum_{\mathbf{q}_1\mathbf{q}_2}\sum_{j_1j_2}\tilde{B}(-\mathbf{q}_1j_1;-\mathbf{q}_2j_2;\mathbf{k}j)[\mathbf{k}\cdot\boldsymbol{\varepsilon}(\mathbf{q}_1j_1)][\mathbf{k}\cdot\boldsymbol{\varepsilon}(\mathbf{q}_2j_2)][\mathbf{k}\cdot\boldsymbol{\varepsilon}(-\mathbf{k}j)]$$
$$\times\int\frac{d\omega_1d\omega_2}{2\pi}\frac{N(-\omega_1)N(-\omega_2)}{N(-\omega)}A_{\mathbf{q}_1j_1}(\omega_1)A_{\mathbf{q}_2j_2}(\omega_2)\delta(\omega-\omega_1-\omega_2). \quad (2.25)$$

Since $A_{\mathbf{k}j}(\omega)$ is peaked at the frequency of the true phonon of wave vector $\mathbf{k}$ and polarization j, its Hilbert transform $I_{\mathbf{k}j}(\omega)$ goes through zero at, and is asymmetrical about, this frequency. In calculating G, the amplitude of this asymmetrical function, we neglect anharmonic effects and replace the spectral function by its harmonic form

$$A_{\mathbf{k}j}(\omega)=(\pi/M\omega_{\mathbf{k}j})[\delta(\omega-\omega_{\mathbf{k}j})-\delta(\omega+\omega_{\mathbf{k}j})]. \quad (2.26)$$

When we substitute Eq. (2.26) into Eq. (2.25) and perform the integrals over ω_1 and ω_2, we obtain the result that

$$G_{kj}(\omega)=\frac{\pi}{2(N)^{1/2}M^2}\sum_{q_1q_2}\sum_{j_1j_2}\frac{\tilde{B}(-\mathbf{q}_1j_1;-\mathbf{q}_2j_2;\mathbf{k}j)}{\omega_{q_1j_1}\omega_{q_2j_2}}[\mathbf{k}\cdot\boldsymbol{\varepsilon}(\mathbf{q}_1j_1)][\mathbf{k}\cdot\boldsymbol{\varepsilon}(\mathbf{q}_2j_2)][\mathbf{k}\cdot\boldsymbol{\varepsilon}(\mathbf{k}j)]$$
$$\times\{[N(\omega_{q_1j_1})+N(\omega_{q_2j_2})+1][\delta(\omega-\omega_{q_1j_1}-\omega_{q_2j_2})-\delta(\omega+\omega_{q_1j_1}+\omega_{q_2j_2})]$$
$$+[N(\omega_{q_1j_1})-N(\omega_{q_2j_2})][\delta(\omega+\omega_{q_1j_1}-\omega_{q_2j_2})-\delta(\omega-\omega_{q_1j_1}+\omega_{q_2j_2})]\}. \quad (2.27)$$

The scattering function $S(\mathbf{k},\omega)$, which describes the one-phonon peak in the scattering cross section, is given by[3,5]

$$S_1(\mathbf{k};\omega)=-(N/2\pi)[d(\mathbf{k})]^2N(-\omega)\sum_j[\mathbf{k}\cdot\boldsymbol{\varepsilon}(\mathbf{k}j)]^2A_{kj}(\omega). \quad (2.28)$$

Combining Eqs. (2.23) and (2.28), we can express the scattering function which describes the one-phonon peak, as well as the interference between the one-phonon peak and the multiphonon background, as

$$S(\mathbf{k},\omega)=(N/2\pi)\frac{[d(\mathbf{k})]^2}{1-e^{-\beta\omega}}\sum_j\{[\mathbf{k}\cdot\boldsymbol{\varepsilon}(\mathbf{k}j)]^2A_{kj}(\omega)-I_{kj}(\omega)G_{kj}(\omega)\}. \quad (2.29)$$

To the lowest nonvanishing order in the anharmonic force constants, the spectral density $A_{kj}(\omega)$ is given by

$$A_{kj}(\omega)=\frac{2}{M}\frac{2\omega_{kj}\Gamma_{kj}(\omega)}{[\omega^2-\Omega_{kj}^2(\omega)]^2+4\omega_{kj}^2\Gamma_{kj}^2(\omega)}, \quad (2.30)$$

where

$$\Omega_{kj}(\omega)=\{\omega_{kj}^2+2\omega_{kj}\Delta_{kj}(\omega)\}^{1/2}$$
$$\approx\omega_{kj}+\Delta_{kj}(\omega)+\cdots, \quad (2.31)$$

and $\Delta_{kj}(\omega)$ and $\Gamma_{kj}(\omega)$ are the frequency-dependent shift and width for which explicit expressions are given in Refs. 4, 5, and 6. The function $I_{kj}(\omega)$, which is the Hilbert transform of $A_{kj}(\omega)$, can be written to the same approximation as

$$I_{kj}(\omega)=\frac{1}{M}\frac{\omega^2-\Omega_{kj}^2(\omega)}{[\omega^2-\Omega_{kj}^2(\omega)]^2+4\omega_{kj}^2\Gamma_{kj}^2(\omega)}. \quad (2.32)$$

Substituting Eqs. (2.30) and (2.32) into Eq. (2.29), we obtain as the starting point for our calculation of $S(\mathbf{k},\omega)$:

$$S(\mathbf{k},\omega)=(N/2\pi)\frac{[d(\mathbf{k})]^2}{1-e^{-\beta\omega}}\sum_j\frac{[\mathbf{k}\cdot\boldsymbol{\varepsilon}(\mathbf{k}j)]^2}{M\omega_{kj}}$$
$$\times\frac{\Gamma_{kj}(\omega)+H_{kj}(\omega)(\omega^2-\Omega_{kj}^2(\omega))/2\omega_{kj}}{[(\omega^2-\Omega_{kj}^2(\omega))/2\omega_{kj}]^2+\Gamma_{kj}^2(\omega)}. \quad (2.33)$$

In writing Eq. (2.33) we have found it convenient to introduce the function

$$H_{kj}(\omega)=-G_{kj}(\omega)/2(\mathbf{k}\cdot\boldsymbol{\varepsilon}(\mathbf{k}j))^2. \quad (2.34)$$

Since the evaluation of $\Delta_{kj}(\omega)$ and $\Gamma_{kj}(\omega)$ has been described in detail in Ref. 6, we omit a discussion of such calculations here and turn now to the evaluation of $G_{kj}(\omega)$ and hence of $H_{kj}(\omega)$.

3. THE EVALUATION OF $H_{kj}(\omega)$

It was decided to evaluate $H_{kj}(\omega)$ in the high-temperature limit because a computer program already exists for the calculation of closely related quantities, the phonon widths and shifts, in this limit.[6] In the high-temperature limit, the mean phonon occupation number can be approximated by

$$N(\omega_{kj})\cong k_BT/\omega_{kj}, \quad (3.1)$$

where k_B is Boltzmann's constant, and the expression for $G_{kj}(\omega)$ can be written in this limit as

$$G_{kj}(\omega)=\frac{\pi\omega k_BT}{2(N)^{1/2}M^2}[\mathbf{k}\cdot\boldsymbol{\varepsilon}(\mathbf{k}j)]\sum_{q_1q_2}\sum_{\pm j_1\pm j_2}\frac{\tilde{B}(-\mathbf{q}_1j_1;-\mathbf{q}_2j_2;\mathbf{k}j)}{\omega_{q_1j_1}^2\omega_{q_2j_2}^2}[\mathbf{k}\cdot\boldsymbol{\varepsilon}(\mathbf{q}_1j_1)][\mathbf{k}\cdot\boldsymbol{\varepsilon}(\mathbf{q}_2j_2)]\delta(\omega-\omega_{q_1j_1}-\omega_{q_2j_2}), \quad (3.2)$$

where we have used the convention that

$$\omega_{q-j}=-\omega_{qj}, \quad (3.3)$$

while none of the other functions in Eq. (3.2) is affected by the replacement $j_i\rightarrow -j_i$.

The coefficient $\tilde{B}(\mathbf{q}_1j_1;\mathbf{q}_2j_2;\mathbf{q}_3j_3)$ takes the following form for our nearest-neighbor, central force model of a face-centered cubic crystal[5]:

$$\tilde{B}(\mathbf{q}_1j_1;\mathbf{q}_2j_2;\mathbf{q}_3j_3)=\frac{8}{N^{1/2}}\frac{\phi'''(r_0)}{2\cdot2^{3/2}}\Delta(\mathbf{q}_1+\mathbf{q}_2+\mathbf{q}_3)F(\mathbf{q}_1j_1;\mathbf{q}_2j_2;\mathbf{q}_3j_3). \quad (3.4)$$

In this expression $\phi(r)$ is the interatomic potential function, and r_0 is the nearest-neighbor separation, while the function $\Delta(\mathbf{q})$ equals unity if $\mathbf{q}$ is 2π times any translation vector of the reciprocal lattice, and vanishes otherwise. The function $F(\mathbf{q}_1 j_1; \mathbf{q}_2 j_2; \mathbf{q}_3 j_3)$ is a real function which is given by

$$F(\mathbf{q}_1 j_1; \mathbf{q}_2 j_2; \mathbf{q}_3 j_3) = \sum_{\mathbf{n}, n.n.} e^{\frac{1}{4}ia_0\mathbf{n}\cdot(\mathbf{q}_1+\mathbf{q}_2+\mathbf{q}_3)}[\mathbf{n}\cdot\boldsymbol{\mathcal{E}}(\mathbf{q}_1 j_1)][\mathbf{n}\cdot\boldsymbol{\mathcal{E}}(\mathbf{q}_2 j_2)][\mathbf{n}\cdot\boldsymbol{\mathcal{E}}(\mathbf{q}_3 j_3)] \sin\frac{a_0}{4}\mathbf{q}_1\cdot\mathbf{n} \sin\frac{a_0}{4}\mathbf{q}_2\cdot\mathbf{n} \sin\frac{a_0}{4}\mathbf{q}_3\cdot\mathbf{n}. \quad (3.5)$$

$\mathbf{n}$ is a dimensionless position vector with integer components which is related to $\mathbf{g}$ by

$$\mathbf{g} = \tfrac{1}{2}a_0\mathbf{n}, \quad (3.6)$$

where a_0 is the lattice parameter, $\sqrt{2}r_0$. The sum in Eq. (3.5) extends over the twelve nearest neighbors of a given atom.

For computational purposes it is essential to work with dimensionless quantities. We accordingly introduce dimensionless frequencies x and $\lambda_{\mathbf{k}j}$ by

$$\omega = 2\omega_L x, \quad (3.7a)$$

$$\omega_{\mathbf{k}j} = \tfrac{1}{2}\omega_L \lambda_{\mathbf{k}j}, \quad (3.7b)$$

where ω_L is the largest normal mode frequency of the crystal. Since the argument of the δ function in Eq. (3.2) cannot vanish if the magnitude of ω exceeds $2\omega_L$, we see from Eq. (3.7) that x is confined to the interval $(-1, 1)$.

We can combine Eqs. (3.2), (3.4), (3.5), and (3.7) to express $G_{\mathbf{k}j}(2\omega_L x)$ as

$$G_{\mathbf{k}j}(2\omega_L x) = -8\sqrt{2}\pi \frac{k_B T}{(M\omega_L{}^2)^2} \phi'''(r_0)(\mathbf{k}\cdot\boldsymbol{\mathcal{E}}(\mathbf{k}j)) \sum_{\alpha\beta} k_\alpha k_\beta g_{\alpha\beta}(\mathbf{k}j; x), \quad (3.8)$$

where

$$g_{\alpha\beta}(\mathbf{k}j; x) = \frac{x}{N} \sum_{\mathbf{q}_1\mathbf{q}_2} \sum_{\pm j_1 \pm j_2} \Delta(-\mathbf{k}+\mathbf{q}_1+\mathbf{q}_2) \frac{F(-\mathbf{k}j; \mathbf{q}_1 j_1; \mathbf{q}_2 j_2)}{\lambda_{\mathbf{q}_1 j_1}{}^2 \lambda_{\mathbf{q}_2 j_2}{}^2} \mathcal{E}_\alpha(\mathbf{q}_1 j_1) \mathcal{E}_\beta(\mathbf{q}_2 j_2) \delta(x - \tfrac{1}{4}\lambda_{\mathbf{q}_1 j_1} - \tfrac{1}{4}\lambda_{\mathbf{q}_2 j_2}). \quad (3.9)$$

To evaluate $g_{\alpha\beta}(\mathbf{k}j; x)$, we expanded it in a series of Legendre polynomials

$$g_{\alpha\beta}(\mathbf{k}j; x) = \sum_{n=1}^{\infty} b_n(\mathbf{k}j; \alpha\beta) P_{2n-1}(x), \quad (3.10)$$

where only the odd order polynomials appear, because from Eq. (3.9) it follows that $g_{\alpha\beta}(\mathbf{k}j; x)$ is an odd function of x. The expansion coefficients are given by

$$b_n(\mathbf{k}j; \alpha\beta) = \frac{4n-1}{2} \int_{-1}^{1} dx g_{\alpha\beta}(\mathbf{k}j; x) P_{2n-1}(x)$$

$$= \tfrac{1}{8} 2(4n-1)\beta_n(\mathbf{k}j; \alpha\beta), \quad (3.11)$$

where

$$\beta_n(\mathbf{k}j; \alpha\beta) = \frac{1}{N} \sum_{\mathbf{q}_1\mathbf{q}_2} \sum_{j_1 j_2} \Delta(-\mathbf{k}+\mathbf{q}_1+\mathbf{q}_2) \frac{F(-\mathbf{k}j; \mathbf{q}_1 j_1; \mathbf{q}_2 j_2)}{\lambda_{\mathbf{q}_1 j_1}{}^2 \lambda_{\mathbf{q}_2 j_2}{}^2} \mathcal{E}_\alpha(\mathbf{q}_1 j_1) \mathcal{E}_\beta(\mathbf{q}_2 j_2)$$

$$\times \left[(\lambda_{\mathbf{q}_1 j_1} + \lambda_{\mathbf{q}_2 j_2}) P_{2n-1}\left(\frac{\lambda_{\mathbf{q}_1 j_1} + \lambda_{\mathbf{q}_2 j_2}}{4}\right) + (\lambda_{\mathbf{q}_1 j_1} - \lambda_{\mathbf{q}_2 j_2}) P_{2n-1}\left(\frac{\lambda_{\mathbf{q}_1 j_1} - \lambda_{\mathbf{q}_2 j_2}}{4}\right) \right]. \quad (3.12)$$

The form of the coefficients given by Eq. (3.11) was chosen in order to make the present calculations parallel those of Ref. 6 as closely as possible. Note that in Eq. (3.12) the branch indices j_1 and j_2 take on positive values only.

In the numerical calculations based on Eqs. (3.8), (3.11), and (3.12), for simplicity the momentum transfer $\mathbf{k}$ was chosen to lie along the [100] direction,

$$\mathbf{k} = [k, 0, 0]. \quad (3.13)$$

All of the results in the remainder of this paper, unless the contrary is stated, are based on Eq. (3.13). Only the polarization vector corresponding to the purely longitudinal mode, which we denote by $j=1$, has a nonvanishing scalar product with $\mathbf{k}$, because

$$\begin{aligned} \boldsymbol{\mathcal{E}}(\mathbf{k}1) &= [1, 0, 0], \\ \boldsymbol{\mathcal{E}}(\mathbf{k}2) &= [0, \sin\theta, \cos\theta], \\ \boldsymbol{\mathcal{E}}(\mathbf{k}3) &= [0, \cos\theta, -\sin\theta], \end{aligned} \quad (3.14)$$

when $\mathbf{k}$ is given by Eq. (3.13). Combining Eqs. (3.11), (3.13), and (3.14) with Eq. (3.8), and recalling the definition of $H_{\mathbf{k}j}(\omega)$, Eq. (2.34), we find that

$$H_{k1}(2\omega_L x)=\left\{\frac{\pi^2}{64}k_B\Theta_\infty\frac{\phi'''(\bar{r}_0)}{\bar{r}_0(\phi''(\bar{r}_0))^2}\right\}\left(\frac{T}{\Theta_\infty}\right)\left(\frac{ka_0}{2\pi}\right)\sum_{n=1}^{\infty}2(4n-1)\beta_n(\mathbf{k}1;xx)P_{2n-1}(x). \tag{3.15}$$

In Eq. (3.15) Θ_∞ is the limiting high-temperature value of the equivalent Debye temperature and is given for the present crystal model by[5]

$$\Theta_\infty=\frac{1}{k_B}\left(\frac{20}{3}\frac{\phi''(\bar{r}_0)}{M}\right)^{1/2}. \tag{3.16}$$

In Eqs. (3.15) and (3.16) the bar over r_0 means that we must use the value of r_0 which corresponds to the minimum of the crystal potential energy. This is because $H_{\mathbf{k}j}(2\omega_L x)$ is already proportional to $\phi'''(r_0)$: the use of the value of r_0 corresponding to the temperature T rather than $\bar{r}_0$ introduces higher order anharmonic corrections to the expression for $H_{\mathbf{k}j}(2\omega_L x)$ than interest us here. In writing Eq. (3.15) we have used the fact that the maximum frequency of the crystal is given by[5]

$$\omega_L^2=8\phi''(\bar{r}_0)/M. \tag{3.17}$$

If we use the values of $\bar{r}_0$ and the potential derivatives given in Ref. 5, which were determined from various properties of lead, the expression in curly brackets on the right side of Eq. (3.15) has the value -0.2573×10^{-2}, while Θ_∞ equals 143.4°K. We therefore obtain, finally, that

$$H_{k1}(2\omega_L x)=-0.2573\times10^{-2}(T/\Theta_\infty)\times(ka_0/2\pi)h_{xx}(\mathbf{k}1;x), \tag{3.18}$$

where

$$h_{xx}(\mathbf{k}1;x)=\sum_{n=1}^{\infty}2(4n-1)\beta_n(\mathbf{k}1;xx)P_{2n-1}(x). \tag{3.19}$$

To give an indication of the accuracy with which we can calculate functions like $h_{xx}(\mathbf{k}1;x)$ by the present methods, in Figs. 1 and 2 we have plotted the function $h_{xx}(\mathbf{k}1;x)$ as a function of x for two different choices of the vector $\mathbf{k}$ lying in the [100] direction. The first 25 coefficients $\{\beta_n(\mathbf{k}1;xx)\}$ were computed from Eq. (3.12) for each value of $\mathbf{k}$, and the values of $h_{xx}(\mathbf{k}1;x)$ were calculated on the basis of the first 24 coefficients and on the basis of all 25 coefficients, at steps of 0.02 in x in the interval (0,1). A grid of 2048 points in the first Brillouin zone for the face-centered cubic lattice was used in these calculations.

From Fig. 1 we see that for the choice $\mathbf{k}a_0=(\pi,0,0)$, which corresponds to half the distance to the Brillouin zone boundary in the [100] direction, the curves for $h_{xx}(\mathbf{k}1;x)$ computed using either the first 24 or the first 25 terms in the expansion (3.10) virtually coincide to the accuracy of our plot. The agreement is less good for the choice $\mathbf{k}a_0=(2\pi,0,0)$ which is on the zone boundary. The two curves shown in Fig. 2, corresponding to the use of the first 24 and 25 terms in the expansion (3.19), however, coincide rather well except in the neighborhood of $x=0$ and $x=1$. The fact that the curves oscillate about each other in these neighborhoods probably means that they are trying to approximate to a smooth and slowly varying function. It should also be pointed out that $h_{xx}(\mathbf{k}1;x)$ goes to zero as x approaches unity, and the failure of our curves to do so is a measure of their inaccuracy in the neighborhood of $x=1$.

The frequency of the longitudinal phonons of wave vector $\mathbf{k}a_0=(\pi,0,0)$ is $x=0.3536$. The frequency of longitudinal phonons with $\mathbf{k}a_0=(2\pi,0,0)$ is 0.5. From Figs. 1 and 2 we see that $h_{xx}(\mathbf{k}1;x)$ is not slowly varying in the neighborhoods of these frequencies. The widths of the one-phonon peak centered at the frequency $\omega=\omega_{\mathbf{k}j}$, as calculated in Ref. 6 for the present crystal model at 425°K, are

$$\begin{aligned}&\mathbf{k}a_0=(\pi,0,0): \quad [2\Gamma_{\mathbf{k}1}(\omega_{\mathbf{k}1})/2\omega_L]=3.12\times10^{-3},\\ &\mathbf{k}a_0=(2\pi,0,0): \quad [2\Gamma_{\mathbf{k}1}(\omega_{\mathbf{k}1})/2\omega_L]=0.6\times10^{-1}.\end{aligned} \tag{3.20}$$

The experimentally determined widths are somewhat larger.[16] The variation of $h_{xx}(\mathbf{k}1;x)$ over this interval is about 15% for $\mathbf{k}a_0=(\pi,0,0)$ and about 100% for $\mathbf{k}a_0=(2\pi,0,0)$. It would, therefore, be a poor approxima-

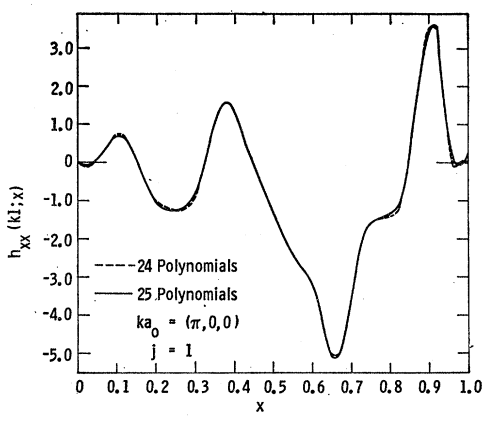

FIG. 1. A plot of the function $h_{xx}(\mathbf{k}1;x)$ which is effectively the strength of the interference term for $\mathbf{k}a_0=(\pi,0,0)$. The index 1 denotes the longitudinal mode, and $x=\omega/2\omega_L$, where ω_L is the maximum frequency of the crystal. The dashed curve gives the result of the calculation in which the first 24 odd Legendre polynomials are used to approximate this function; the solid curve gives the result when the first 25 odd Legendre polynomials are used. A nearest-neighbor, central force model of a face-centered cubic crystal chosen to approximate lead, was used in these calculations.

[16] B. N. Brockhouse, T. Arase, G. Caglioti, M. Sakamoto, R. N. Sinclair, and A. D. B. Woods, *Inelastic Scattering of Neutrons in Solids and Liquids* (International Atomic Energy Agency, Vienna, 1961), p. 531.

tion to replace $H_{kj}(\omega)$ by its value at $\omega=\omega_{kj}$ in the latter case in computing the line shape function $S(\mathbf{k},\omega)$, and we have not done so in the calculations described in the next section.

4. THE FUNCTION $S(\mathbf{k},\omega)$

To calculate the scattering function $S(\mathbf{k},\omega)$ given by Eq. (2.33) we first express it in terms of dimensionless quantities. If we use the dimensionless frequencies introduced in Eq. (3.7), together with the definitions

$$\delta_{kj}(x)=\Delta_{kj}(2\omega_L x)/\omega_L, \tag{4.1a}$$

$$\gamma_{kj}(x)=\Gamma_{kj}(2\omega_L x)/\omega_L, \tag{4.1b}$$

we obtain

$$S(\mathbf{k},2\omega_L x)=\frac{N}{\pi M\omega_L{}^2}\frac{[d(\mathbf{k})]^2}{1-e^{-2\beta\omega_L x}}\sum_j\frac{(\mathbf{k}\cdot\boldsymbol{\varepsilon}(\mathbf{k}j))^2}{\lambda_{kj}}\frac{\gamma_{kj}(x)+H_{kj}(2\omega_L x)[4x^2-(\frac{1}{2}\lambda_{kj}+\delta_{kj}(x))^2]/\lambda_{kj}}{[[4x^2-(\frac{1}{2}\lambda_{kj}+\delta_{kj}(x))^2]/\lambda_{kj}]^2+\gamma_{kj}{}^2(x)}, \tag{4.2}$$

$$=\frac{N}{\pi M\omega_L{}^2}\frac{[d(\mathbf{k})]^2}{1-e^{2\beta\omega_L x}}\sum_j\frac{(\mathbf{k}\cdot\boldsymbol{\varepsilon}(\mathbf{k}j))^2}{\lambda_{kj}}s_{kj}(x). \tag{4.3}$$

Equations (4.2) and (4.3) define the function $s_{kj}(x)$, and it is with this function that we will be concerned in the remainder of this paper.

In the present calculations we wrote the frequency-dependent shift $\delta_{kj}(x)$ as the sum of three contributions,

$$\delta_{kj}(x)=\delta_{kj}{}^{(T)}+\delta_{kj}{}^{(4)}+\delta_{kj}{}^{(3)}(x). \tag{4.4}$$

In this expression $\delta_{kj}{}^{(T)}$ is the shift in the phonon frequency from its value in the strict harmonic approximation due to thermal expansion. It has been discussed in Refs. 5 and 7. (By strict harmonic approximation we mean the approximation in which the crystal potential energy is expanded to quadratic terms in the displacements of the atoms from their equilibrium positions in the atomic configuration which corresponds to the minimum of the potential, rather than free, energy.) The contribution $\delta_{kj}{}^{(4)}$ is the contribution to the shift from the quartic anharmonic terms in first-order perturbation theory. Note that although $\delta_{kj}{}^{(T)}$ and $\delta_{kj}{}^{(4)}$ are functions of $\mathbf{k}$ and j as well as of the temperature, they are independent of x. The explicit expressions for $\delta_{kj}{}^{(T)}$ and $\delta_{kj}{}^{(4)}$ used in the present calculations are[5]

$$\delta_{kj}{}^{(T)}=-0.01930(T/\Theta_\infty)\lambda_{kj}, \tag{4.5a}$$

$$\delta_{kj}{}^{(4)}=0.01501(T/\Theta_\infty)\lambda_{kj}, \tag{4.5b}$$

with

$$\lambda_{k1}=2\sin(a_0k/4), \tag{4.6}$$

for $\mathbf{k}$ given by Eq. (3.13). The last term $\delta_{kj}{}^{(3)}(x)$ is the contribution to the shift from the cubic anharmonic terms in second-order perturbation theory.

The functions $\delta_{kj}{}^{(3)}(x)$ and $\gamma_{kj}(x)$ have the following expansions in the high-temperature limit for the model of a face-centered cubic crystal used in the preceding section for the evaluation of $H_{kj}(2\omega_L x)$:

$$\delta_{kj}{}^{(3)}(x)=6.035\times10^{-4}\frac{1}{\lambda_{kj}}\times\left(\frac{T}{\Theta_\infty}\right)\sum_{n=1}^{\infty}2(4n-1)\alpha_n(\mathbf{k}j)Q_{2n-1}(x), \tag{4.7a}$$

$$\gamma_{kj}(x)=6.035\times10^{-4}\frac{\pi}{2\lambda_{kj}}\times\left(\frac{T}{\Theta_\infty}\right)\sum_{n=1}^{\infty}2(4n-1)\alpha_n(\mathbf{k}j)P_{2n-1}(x), \tag{4.7b}$$

where $P_\nu(x)$ and $Q_\nu(x)$ are Legendre's functions of the first and second kind for x in the interval $(-1, 1)$, and where the coefficient $\alpha_n(\mathbf{k}j)$ is given explicitly in Ref. 6. The principal difference between the present calculations of $\delta_{kj}{}^{(3)}(x)$ and $\gamma_{kj}(x)$ and those described in Ref. 6 is that the computer program for the evaluation of the $\{\alpha_n(\mathbf{k}j)\}$ was rewritten to allow a larger number of these coefficients to be calculated, and a subroutine was added for printing out the values of $\delta_{kj}{}^{(3)}(x)$ and $\gamma_{kj}(x)$ as a function of x.

In Figs. 3 and 4 we have plotted $\tilde{\gamma}_{kj}(x)=\gamma_{kj}(x)/$

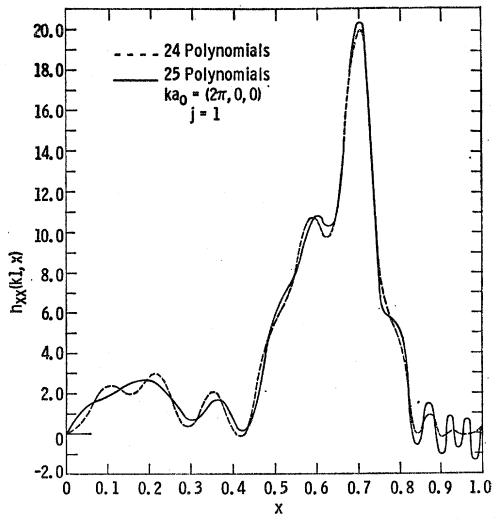

FIG. 2. A plot of the function $h_{xx}(\mathbf{k}1;x)$ for $\mathbf{k}a=(2\pi,0,0)$. The various labels in the figure have the same meanings here as in Fig. 1.

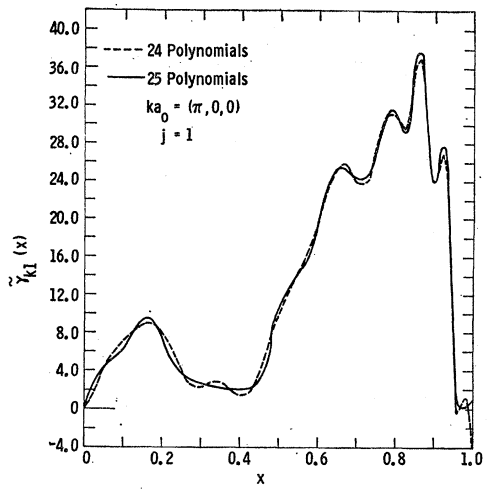

FIG. 3. A plot of the function $\tilde{\gamma}(\mathbf{k}1;x)$, which is effectively the half-width of the one-phonon peak, for $\mathbf{k}a_0=(\pi,0,0)$. The captions have the same meaning here as in Fig. 1.

$[6.035\times10^{-4}(\pi/2\lambda_{kj})(T/\Theta_\infty)]$ for $j=1$ and for $\mathbf{k}a_0=(\pi,0,0)$ and $(2\pi,0,0)$, respectively. In each case we have plotted the approximation to $\tilde{\gamma}_{k1}(x)$ obtained using 24 and 25 terms in the expansion (4.7b) which defines this function. Again we see that although there are some differences between the curves obtained using 24 and 25 Legendre polynomials, the agreement is sufficiently good that it appears that the appreciable structure displayed by this function is genuine. Figures 3 and 4, however, display one disadvantage of approximating functions like $h_{xx}(\mathbf{k}1;x)$, $\delta_{kj}^{(3)}(x)$, and $\gamma_{kj}(x)$ by expansions in a finite number of Legendre functions. We see from Fig. 4 that $\tilde{\gamma}_{k1}(x)$ is negative in the neighborhood of $x=0.4$. From Figs. 3 and 4 we also see that in the present approximation $\tilde{\gamma}_{k1}(x)$ is negative in the neighborhood of $x=1$. From the explicit form of $\gamma_{kj}(x)$[5,6] it can be seen that it is a non-negative function of x in the interval (0,1). How many more terms in the expansion of $\tilde{\gamma}_{k1}(x)$ would be required to yield a non-negative result is not known. In the calculations in which it was used, the function $\tilde{\gamma}_{k1}(x)$ shown in Fig. 4 was set equal to zero in the region around $x=0.4$ where it becomes negative. The rapid oscillations in $\tilde{\gamma}_{k1}(x)$ for x close to 1 probably mean that the function is very slowly varying in this region, because the oscillations are out of phase in successive approximations. As a practical matter, the behavior of $\tilde{\gamma}_{k1}(x)$ in the neighborhood of $x=1$ is unimportant, at least in the present calculations, because, as we will see below, the function $s_{k1}(x)$ is essentially zero in this region.

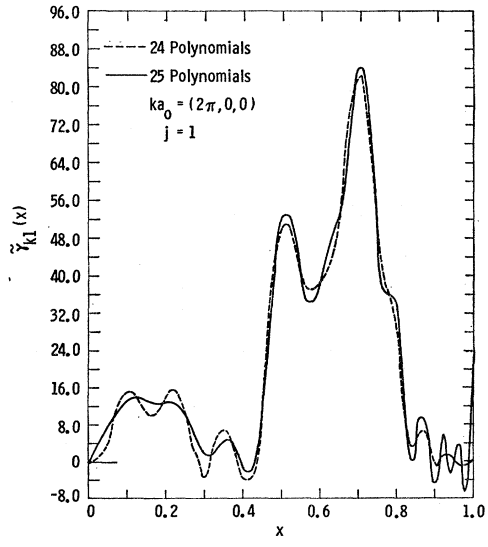

FIG. 4. A plot of the function $\tilde{\gamma}(\mathbf{k}1;x)$ for $\mathbf{k}a_0=(2\pi,0,0)$. The various labels in the figure have the same meaning here as in Fig. 1.

In Figs. 5 and 6 we have plotted $s_{k1}(x)$ as a function of x for $\mathbf{k}a_0=(\pi,0,0)$ and $\mathbf{k}a_0=(2\pi,0,0)$, respectively, at a temperature of 425°K. In these two figures the vertical scale is magnified so that the contribution of the asymmetric interference term to $s_{k1}(x)$ is more easily seen. The 25 polynomial approximations to all the x-dependent functions were used in these calculations. In each of these figures the dashed curve gives the form of $s_{k1}(x)$ when the interference term is omitted from the calculation, while the solid curve gives the form of $s_{k1}(x)$ when it is included. Because $H_{k1}(2\omega_L x)$ is negative both below and above the resonance frequency for $\mathbf{k}a_0=(\pi,0,0)$, as can be seen from Fig. 1, while it is always positive for $\mathbf{k}a_0=(2\pi,0,0)$ (Fig. 2), there is a qualitative difference between the effects of the interference term in the two cases which would not have been predicted if we had ignored the frequency dependence of $H_{k1}(2\omega_L x)$ and had approximated it by its value at the resonance frequency. In the former case, the interference term depresses both the left- and right-hand wings of the resonance peak near the center of the peak, while

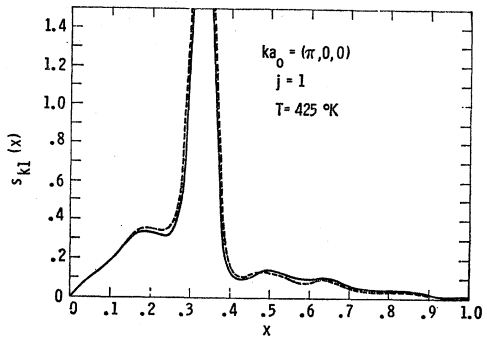

FIG. 5. A plot of the scattering function $s_{k1}(x)$ for $\mathbf{k}a_0=(\pi,0,0)$, in the neighborhood of the center of the line. The dashed curve gives the form of $s_{k1}(x)$ when the interference term is omitted from the calculation; the solid curve gives the form of this function when the interference term is included. All of the functions entering into the definition of $s_{k1}(x)$ were computed in the 25 Legendre function approximation. The crystal temperature was taken to be 425°K.

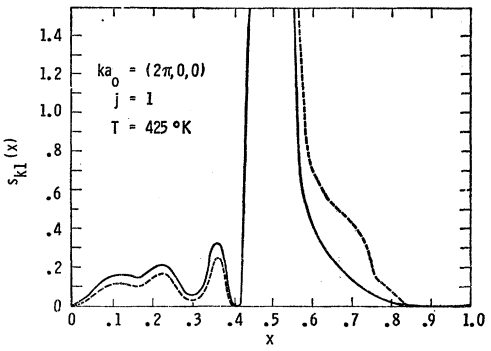

FIG. 6. A plot of $s_{k1}(x)$ for $\mathbf{k}a_0=(2\pi,0,0)$, in the neighborhood of the center of the line. The explanation of the plot is the same as in Fig. 5.

in the latter case the left-hand side of the curve is raised and the right-hand side is depressed. (In fact the interference term does also raise the right-hand side of the former curve close to the center of the resonance, but this could not be shown in Fig. 3 on the scale to which it is drawn.) Although, on a relative basis, the effects of the interference term are appreciable in the wings of the resonance curves, on an absolute basis, the results of the present calculation suggest that they are quite small, because the function $s_{k1}(x)$ itself is already small for those values of x for which the interference term makes its largest contribution. The effects of the interference term probably lie well outside the limits of observability attainable by presently available reactors.

In Figs. 7 and 8 we have replotted $s_{k1}(x)$ as a function of x on a more convenient scale for $\mathbf{k}a_0=(\pi,0,0)$ and $\mathbf{k}a_0=(2\pi,0,0)$, respectively, for a temperature of 425°K.

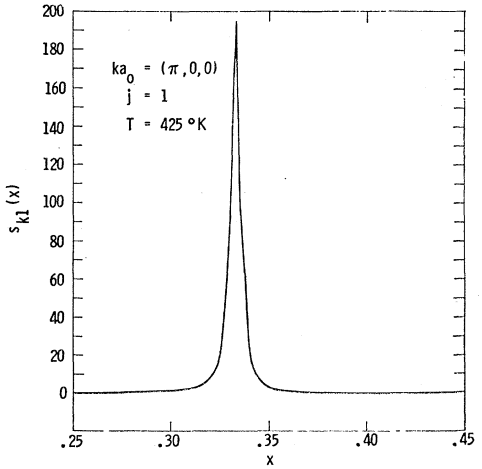

FIG. 7. A plot of $s_{k1}(x)$ for $\mathbf{k}a_0=(\pi,0,0)$ at 425°K.

It is particularly apparent from the result plotted in Fig. 8 that a simple Lorentzian approximation to $s_{k1}(x)$ would be unsatisfactory. This conclusion is also reached by Cowley[11] on the basis of his calculations of what is effectively $s_{kj}(x)$, for $\mathbf{k}=0$.

The widths at half-maximum of the peaks shown in Figs. 7 and 8 are approximately 5.5×10^{-3} and 0.125×10^{-1}, respectively. The first value is somewhat greater than, and the second value is somewhat smaller than, the corresponding values quoted in Eq. (3.20). These differences may be due to our use of more Legendre polynomials in the expansions of $\Gamma_{kj}(\omega)$ and $\Delta_{kj}(\omega)$ in the present calculations and to the fact that the frequency dependences of these functions have been retained in the present calculations.

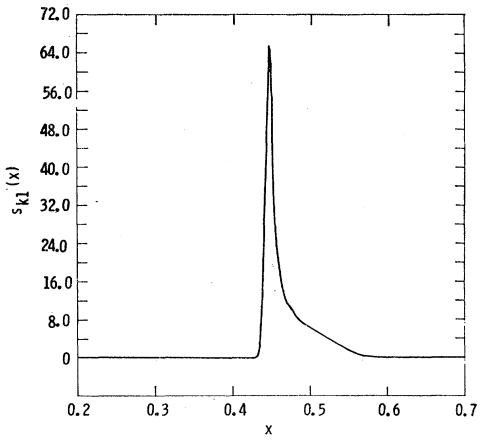

FIG. 8. A plot of $s_{k1}(x)$ for $\mathbf{k}a_0=(2\pi,0,0)$ at 425°K.

Unfortunately, there are no experimental determinations of the line shapes for the scattering of neutrons by longitudinal phonons propagating in the [100] direction in lead, so that comparisons between our theoretical results and experiment cannot be made at the present time. This may be fortunate, in view of the simplicity of our model of lead. However, it also seems to be true that in view of the experimental difficulties encountered in making such measurements, such as the need for high flux reactors and very good instrumental resolution, and the problems encountered in correcting the raw data for the multiphonon background, it will be some while yet before such comparisons become possible.

ACKNOWLEDGMENT

The authors should like to thank Brenda J. Kagle for programming all of the calculations reported in this paper, as well as for helping to prepare the figures.